Thin Solid Films 550 (2014) 732–737

Contents lists available at ScienceDirect

Thin Solid Films

journal homepage: www.elsevier.com/locate/tsf

Inhibition of hydrogen absorption in bulk Pd by the formation of Ru–Pd surface alloy

P. Ferrari, D.E. Diaz-Droguett, S. Rojas, A.L. Cabrera *

Laboratorio de Ciencia de Materiales, Instituto de Física, Pontificia Universidad Católica de Chile, Santiago, Chile

ARTICLE INFO

Article history:
Received 30 July 2013
Received in revised form 29 October 2013
Accepted 31 October 2013
Available online 8 November 2013

Keywords:
Palladium
Ruthenium
Hydrogen
Absorption
Quartz crystal microbalance
Films
Thermal desorption
Auger spectroscopy

ABSTRACT

Thermal programmed desorption (TPD) of hydrogen was performed in Pd and 5% Ru–Pd foils. The foils were inspected with Auger Electron Spectroscopy and Ar ion-sputter cleaned. Hydrogen dosage was 1000 L at 10^{-3} Pa. Hydrogen evolving from Pd (TPD curves) was 12 times larger than for the 5% Ru–Pd foil. A 1.8 μm thick Ru–Pd surface alloy was grown on the surface of Pd and the TPD curves were very similar to those of the 5% Ru–Pd bulk alloy. The lattice parameter of the Pd fcc crystal structure decreased by 2.8%, when alloying with 5% Ru. The lattice parameter of the fcc cell of Pd increased by 2.3% when absorbing hydrogen. Hydrogen saturation amount at 4655 Pa was obtained using a quartz crystal microbalance in a 24 nm Pd film and in a 5% Ru–Pd film. A hydrogen–metal ratio (x = H/Pd) was calculated from these measurements yielding a ratio of $x_{Pd} = 0.68$ for Pd and $x_{RuPd} = 0.27$ for ~2% Ru–Pd film.

1. Introduction

The absorption of hydrogen by bulk Pd has been extensively studied and it is well understood. There are many reviews written which deals with the subject [1,2]. Pd was used as the first commercial solid membrane for many hydrogen applications such as hydrogen purification, tritium separation and dehydrogenation reactions [3]. Pd absorbs large amounts of hydrogen: hydrogen atoms located in octahedral interstitial sites in the Pd face centered cubic conventional cell, allowing theoretically, 4 H per 4 Pd atoms in the cell. This corresponds to atomic ratio of H/Pd = 1. The absorption proceeds without the need for high pressures (from 10^{-4} to 10^{5} Pa) or high temperatures (from 150 to 300 K) thus requiring a very small activation energy for the absorption process [4]. Hydrogen is released from Pd by just removing the hydrogen atmosphere from Pd without spending additional energy, in other words, by a pressure "swing". One important drawback associated with the use of Pd in any industrial application is the high cost and scarcity of this metal and mechanical fatigue under absorption/desorption pressure cycles. Pd cluster-assembled films could be made using small amounts of Pd and could become an alternative to bulk Pd for many applications. High absorption capacity through modification of other cluster-assembled metal or alloy films is possible as shown in our results studying Nb clusters-assembled films [5]. Alloying Pd with other transition metals results detrimental to the hydrogen absorption capacity. We have observed from thermal programmed desorption (TPD) experiments that alloying Pd with 5% Ru decreases greatly the absorption capacity of Pd [6]. Alloying Pd with 17% Ag causes similar effects [6]. Alloying Pd with Nb in metallic clusters also decreased the high absorption capacity of Pd clusters [5]. Other works have also shown this detrimental effect with regard to hydrogen absorption when alloying Pd with Au and Pt [7]. In Ref. [7], it is shown that the absorption capacity of Pd decreases by 13% when alloying Pd with 11% Au and a decrease in absorption capacity of 27% when alloying Pd with 19% Au. In the case of Pt, 9% Pt decreases the absorption capacity by 47% and 19% Pt decreases the hydrogen absorption capacity of Pd by 76%.

In order to understand the decrease in hydrogen absorption capacity by a Pd alloy, scientists have postulated an "electronic" or a "geometric" reason [8]. A geometric reason is easier to grasp since a contraction in the Pd alloy lattice parameter increases the diffusion constant of hydrogen in the lattice and might also decrease the volume available for the interstitial sites. The "electronic" effect was simulated using density-functional calculation [8] for a Pd alloy with fcc structure and with the composition of Pd_3M where M is a metal including Ru, Au, Pt and Ag among others. The main purpose of this work [8] was to understand why the maximum hydrogen solubility in Pd–Ag system was reached when the alloy had the composition Pd_3Ag. For this composition they found that the hydrogen absorption energy was more negative than for pure Pd. They also found a linear relationship (with negative

* Corresponding author.
E-mail address: acabrera@fis.puc.cl (A.L. Cabrera).

0040-6090/$ – see front matter © 2013 Elsevier B.V. All rights reserved.
http://dx.doi.org/10.1016/j.tsf.2013.10.181

slope) between the hydrogen absorption energy and the binding energy for the Pd_3M alloy. In the case of Pd_3Ru the hydrogen absorption energy is positive (0.3 eV per H atom) indicating an unfavorable absorption, but a negative hydrogen absorption energy for Pd_3Au and Pd_3Ag lower than the absorption energy for pure Pd contradicts the experimental results already mentioned here [6,7].

In this research, our goal was to better understand the dramatic decrease in hydrogen absorption capacity for a Ru–Pd alloy. Our study focused on a Pd alloy containing a very small amount of Ru, less than 5%. Thermal programmed desorption of hydrogen in Pd and Pd alloys gives us only kinetic information on the hydrogen–metal absorption/desorption process. Thus we are complementing those results with hydrogen-loading in the metal foils or films measured by change of resistance of the films and also determining the ratio H/M during absorption using a Quartz-Crystal Microbalance (QCM).

The QCM is customarily used inside a film evaporator system to measure minute amounts of material deposited in order to form thin metal films. In particular, the detection of condensed nitrogen to determine roughness and porosity in carbon and magnetic films was reported by Wang, Krim and Toney [9]. The adsorption of a monolayer of liquid nitrogen detected by QCM was also reported by Krim et al. [10]. The detection of a mass amount corresponding to a monolayer of Kr in an area of about 0.5×10^{-4} m^2 [10] encouraged us to implement a QCM system in a modified vacuum chamber to measure the mass amount of hydrogen absorbed by Pd–Ru alloy films. The hydrogen mass absorbed by this method does not give an absolute mass number because two effects are present during absorption from H_2 gas: "environmental pressure stress" and "film stress effect" [11,12]. The first effect is caused by the H_2 total pressure during absorption and the second effect is caused by the expansion of the Pd film due to hydrogen absorption to the quartz crystal. It is well accepted that the shift in the resonant frequency, during gas absorption, is small compared with absorption measurements from a liquid phase. Krim and Daly discussed in chapter D4.0 from the Handbook of Thin Process and Technology that a shift in frequency of 2 Hz was measured due to the stress caused by the typical gold film used as electrode in a 5 MHz quartz crystal when it was submerged in liquid nitrogen (77 K) due to the difference in thermal expansion from the gold and the quartz. For the first effect, using the equation shown in the abovementioned handbook, we calculated that the shift was due to the hydrogen pressure (4500 Pa) and resulted in less than 0.98 Hz. In the case of liquid contact measurements, the main effect which produced a large shift in the resonant frequency of the quartz crystal is the viscous loading [12, page 17]. Depending of the liquid medium, a shift of about 800 Hz could be observed due to this effect. The shift in resonant frequency, due to different effects in liquid contact measurements, was well studied by Czerwinski's research group [13,14] and they found that the shift of the resonant frequency of the QCM yields a hydrogen mass number 3 times greater than the hydrogen amount inferred by the electrochemical current. The absorption capacity of a pure Pd film (film thickness about 10^{-6} m) measured in their work was reported to be H/M around 0.72 and agrees well with our own prior measurements of absorption in Pd films from gas phase of H/M about 0.7 for 45 nm thick Pd films [15].

Our QCM measurements, discussed in the present paper, will be displayed as a H/M ratio, keeping in mind that this is not an absolute number but will serve the purpose of comparison between one system an another. In the case of 5% Ru–Pd alloy, the expansion of the Pd containing film will be smaller because hydrogen absorption is significantly decreased and thus the shift in frequency due to the stress shall be more important in the pure Pd film.

In this work we will describe a procedure to make a Ru–Pd surface alloy, characterization of the alloy with Auger Electron Spectroscopy (AES) and X-ray diffraction (XRD), followed by measurements of hydrogen desorption from the alloy using TPD and hydrogen absorption in equilibrium using the QCM.

2. Experimental details

2.1. Materials

A piece of high purity – 0.2 mm thick – Pd foil with 1.5×10^{-4} m^2 area was obtained from Goodfellow. A foil of 0.025 mm thick of the nominal 5% Ru–Pd alloy (5.45×10^{-4} m^2 total area) was specially ordered from Johnson-Matthey. Evaporation of Pd and Ru metals was done by e-beam-evaporation using a Tectra mini e-beam evaporator [16]. A Pd wire 99.95% purity and Ru ingots were purchased from ESPI Metals. Typically, metals were evaporated at a rate between 0.0003 and 0.007 nm/s and at a pressure of ~1.7×10^{-4} Pa.

2.2. Characterization

2.2.1. X-ray diffraction (XRD) and Grazing Incidence X-ray Diffraction (GID)

All these measurements were done with a Bruker D8 Advance diffractometer equipped with an X-ray tube with a Cu anode (Cu-K_α radiation-$\lambda = 0.154$ nm). Metal foils were characterized and their lattice constants were obtained from X-ray diffraction (XRD) in the usual θ–θ geometry and also with grazing incidence of the X-rays.

2.2.2. Scanning electron microscopy (SEM) with energy dispersive spectroscopy (EDS)

Samples as received and after hydrogen uptake were inspected with scanning electron microscopy using a LEO VP1400 system equipped with energy dispersive spectroscopy. Microscopic images were obtained by operating the SEM at an accelerating voltage of 25 kV and using secondary and back-scattered electron detectors.

2.2.3. Auger Electron Spectroscopy (AES)

AES of the foils was performed before and after their exposure to the hydrogen gas and also after heating for thermal desorption. The analyses were performed with a double-pass cylindrical mirror analyzer system (DESA 100) from Staib Instruments. The primary electron beam was accelerated to 3 kV with an electron current of 0.07 μA. Energy range 100–550 eV and base pressure in the ultra high vacuum (UHV) system was 1.3×10^{-6} Pa More details of the vacuum system are found in the next experimental section.

2.3. Thermal programmed desorption (TPD) measurements

An all stainless steel UHV chamber from MDC-Vacuum Inc. which has a volume of approximately 4×10^{-2} m^3 and pumped by an Adixen 0.15 m^3/s Turbo pump, backed by a rotary pump, was used for the TPD experiments. The UHV system incorporated a double-pass cylindrical mirror analyzer system (DESA 100) from Staib Instruments, a mass spectrometer (RGA 200) from Stanford Research Systems and Ar^+ sputtering ion source (IQE 11/35) from Specs. A home-built manipulator was used to perform the TPD experiments. The manipulator is mounted on a rotary feedthrough from MDC-Vacuum which has two degrees of freedom for motion: it can rotate in 360° and it translates up and down in a range of 2.54×10^{-2} m. Two rigid Cu bars, 0.635×10^{-2} m in diameter, are used for resistively heating the sample foils. The bars are supported by a piece of Macor ceramic. The samples (foils) were directly fixed to the Macor ceramic using all stainless steel screws and a chrome-alumel thermocouple was soldered to the foils to feedback the temperature controller (Eurotherm 2404).

2.4. Hydrogen uptake measured with a Quartz-Crystal Microbalance (QCM)

A QCM system from MDC model SQM-160 was used for the hydrogen absorption measurements. The quartz crystals (that were fitted in

the QCM head) were AT cut from a single crystal, are 1.4×10^{-2} m in diameter and 0.6×10^{-3} m in thickness and oscillate in a transverse shear motion with a resonant frequency between 5 and 6 MHz when bare. The QCM head was placed inside a small (less than 10^{-3} m^3 in volume) all stainless steel vacuum chamber pumped by a 0.05 m^3/s turbo pump from Balzers. A gate valve was placed between the steel chamber and the turbo pump to isolate the chamber from the vacuum, thus making it possible to pressurize with hydrogen gas through a leak valve. The base pressure of the chamber was 1×10^{-4} Pa before hydrogen was admitted. High pressures (in the range of 133 to 10^5 Pa) were measured with a capacitor manometer (Baratron from MKS Instruments).

3. Results and discussion

3.1. Hydrogen TPD in Pd and Pd alloy foils

3.1.1. Pure Pd

An elemental composition on the surface of the pure Pd foil was performed with AES. Two surface contaminants are presented on the "as received" Pd foils: carbon and oxygen. Carbon is due to the typical adventitious carbon present in the UHV before sputtering the foil and oxygen is due to a native oxide present in Pd. After heating in vacuum, sulfur impurities which are normally present in the bulk of Pd in very small concentrations segregate to the surface. Sulfur impurities are very hard to eliminate but they do not interfere much with the hydrogen absorption. AES spectrum of Pd foil after 3 cycles of Ar^+ sputtering is displayed in Fig. 1. After this cleaning procedure, the foil was dosed with 1000 L of hydrogen and a TPD curve was obtained.

3.1.2. 5% Ru–Pd alloy

An elemental composition on the surface of the 5% Ru–Pd foil was obtained with AES. Two surface contaminants are present on the "as received" foils: carbon and oxygen. After heating in vacuum, sulfur impurities also segregated to the surface on this sample. A typical AES spectrum of 5% Ru–Pd is shown in Fig. 2. In spite of the C, and S impurities still present on the surface, one can distinguish a Ru Auger line between a Pd and a C line. Ar^+ sputtering was performed until C and S contaminants were significantly reduced and a hydrogen TPD curve was obtained after a 1000 L dosage.

3.1.3. Ru–Pd surface alloy

8 nm of Ru was e-beam evaporated on the surface of a Pd foil at an almost constant rate of 0.007 nm/s. The foil was placed in the manipulator of the UHV and heated at different temperatures and the elemental composition was determined by AES. The AES spectra obtained right after evaporation of the Ru on the surface of Pd showed that Ru is the predominant element in addition to C contamination. The foil was heated up to 973 K by steps of 50 K and AES was obtained after each heating step. The Ru AES peak at 231 eV and the Pd AES peak at 330 eV were used to calculate surface elemental concentration and this is plotted as a function of temperature in Fig. 3. In this figure one can see that the Ru starts diffusing into the Pd above 773 K and at 973 K, the predominant element on the surface is Pd. After this last heating step, an AES spectrum was taken (shown in Fig. 4) and the Ru atomic surface concentration was calculated to be 5 at.%. At this point the sample was dosed with 1000 L of hydrogen and a TPD curve was obtained. The three TPD curves are displayed in Fig. 5.

The hydrogen released from pure Pd is about 12 times larger than in the 5% Ru–Pd bulk alloy. The amount of hydrogen released from the Ru–Pd surface alloy is very similar to the hydrogen released from the 5% Ru–Pd bulk alloy indicating that this surface alloy is an effective diffusion barrier for hydrogen atoms.

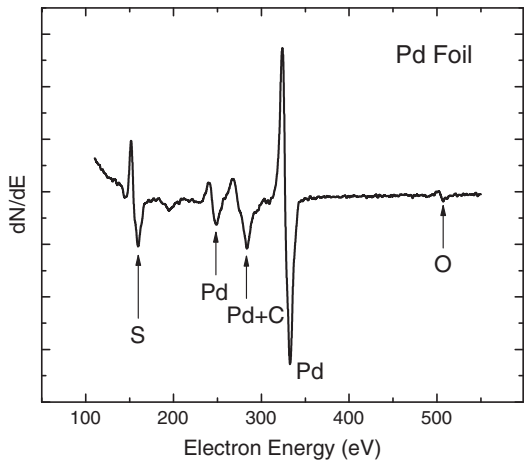

Fig. 1. Typical AES spectra of a Pd foil after 3 cycles of Ar^+ sputtering and heating.

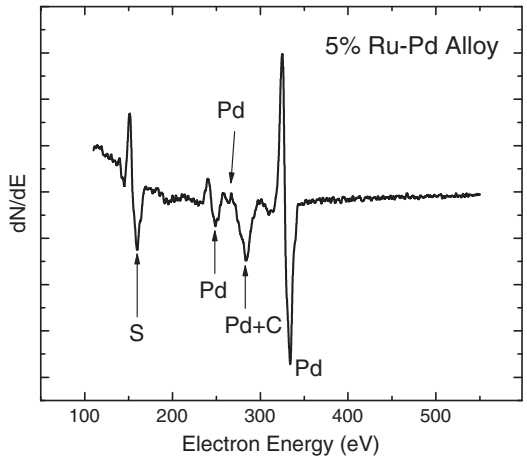

Fig. 2. Typical AES spectrum of 5% Ru–Pd after 3 cycles of Ar^+ sputtering and heating.

3.2. XRD and EDS characterization of foils

3.2.1. Pure Pd

The XRD pattern of Pd foil was obtained at room temperature in air. Diffraction peaks corresponding to planes with Miller indexes (111), (200), (220) and (311) were obtained, being that corresponding to (220) plane the strongest peak which indicates a preferred orientation

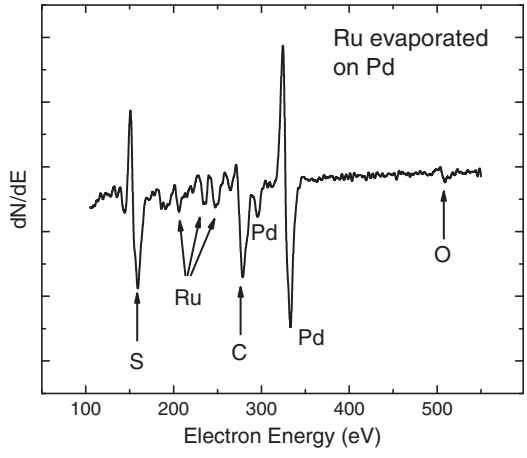

Fig. 3. Plot of Ru and Pd atomic concentration in the Ru–Pd surface alloy as a function of annealing temperature. The Ru AES peak at 231 eV and the Pd AES peak 330 eV were used to calculate atomic concentrations.

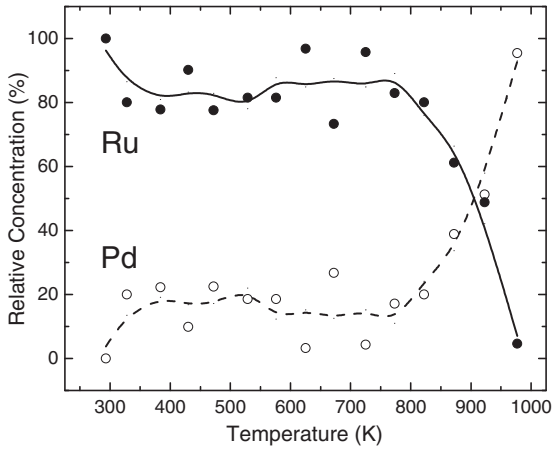

Fig. 4. AES spectrum of the Ru–Pd surface alloy after last heating step for annealing, Ru atomic surface concentration was calculated to be about 5 at.%.

of the foil. The crystal structure of Pd is fcc with a lattice parameter of 0.389 nm.

3.2.2. 5% Ru–Pd alloy

The XRD pattern of the 5% Ru–Pd bulk alloy was obtained under the same conditions as pure Pd foil. Diffraction peaks corresponding to planes with Miller indexes (111), (200), (211), (220), (311) were obtained. In this case, peaks corresponding to planes (200) and (311) look more prominent than in the case of pure Pd foil. The peak corresponding to (220) plane is still the strongest indicating a preferential orientation. The crystal structure is fcc with a lattice parameter of 0.378 nm.

3.2.3. Ru–Pd surface alloy

Grazing Incidence X-ray Diffraction (GID) was performed on both sides of the foil after the TPD experiments. The side in where Ru was e-beam evaporated was labeled "top" and the side with just Pd was labeled "bottom". These GIDs are shown in Fig. 6. The GID corresponding to "top" clearly shows the pattern corresponding to a Ru–Pd alloy with fcc structure and a lattice constant of 0.378 nm. This GID also shows that hydrogen is more effectively retained on this side of the foil. The lattice parameter of PdH_x is 0.398 nm which corresponds to 2.3% of volume expansion of Pd.

All the samples were inspected with SEM and in general the surface looked smooth at ×1000 and ×5000 magnification. EDS was performed in several zones of the samples and three different electron energies

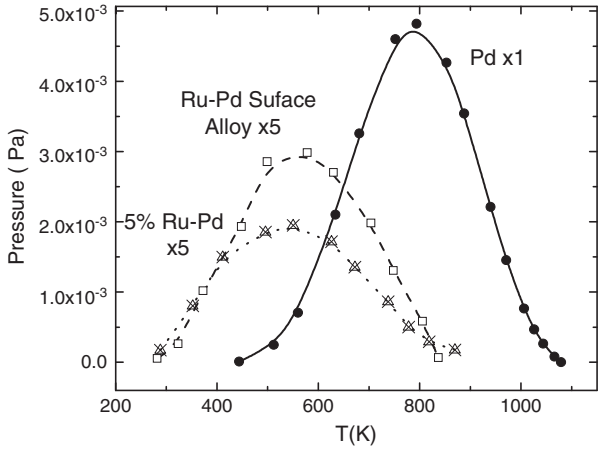

Fig. 5. TPD curves for the three samples studied after dosing with 1000 L of hydrogen: filled circles correspond to Pd foils; open squares correspond to Ru–Pd surface alloys; open triangles correspond to the bulk 5% Ru–Pd alloy.

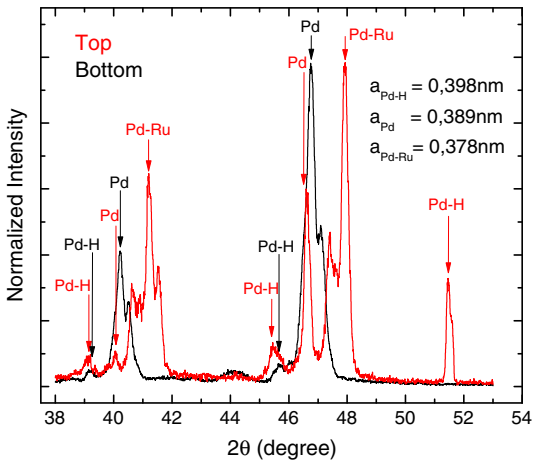

Fig. 6. Grazing Incidence X-ray Diffraction (GID) performed on both sides of the Ru–Pd surface alloy foil after the TPD experiments. The side where Ru was e-beam evaporated was labeled "top" and the side with just Pd was labeled "bottom".

were used in the case of the Ru–Pd surface alloy. The electron energies used were 10, 15 and 25 keV and using the Kanaya–Okayama approximation [17] we estimated the depths of the EDS analyses, being 0.4, 0.8 and 1.8 μm respectively for the three energies. The atomic concentrations are listed in Table 1 for the three samples. In the case of the Ru–Pd surface alloy two different zones were observed, a very smooth one which was predominant on the whole sample, and a rougher one. The rougher zone was richer in Ru concentration indicating an incomplete alloying with Pd in those areas. EDS of the smooth area is listed in Table 1. From these data one can see that Ru in the alloy did not diffuse deeper than 1.8 μm in Pd.

3.3. Hydrogen penetration depth in the foils determined by electrical resistance changes of the foils

It is well established that hydrogen absorption in Pd films increases their electrical resistance [18]. This is due to a resistivity increase in the Pd–H system because H atoms in interstitial sites act as a scattering center for the conduction electrons. Assuming that the time scale for hydrogen adsorption (τ_{ads}) is much faster than the time scale for hydrogen diffusion (τ_{dif}), a hydrogen concentration profile in Pd can be represented by exponential decays as a function of depth. A profile of concentration having this exponential dependence was experimentally measured in Nb films [19]. The concentration can be written in the following form:

$$C(H) = C_0 e^{-z/\lambda(t)}. \quad (1)$$

Where the variable z is the depth into the foil and $\lambda(t)$ is a characteristic penetration length for hydrogen. We can also assume a linear relationship between hydrogen concentration and the resistivity change [18,20] which can be expressed as follows:

$$\Delta\rho = \kappa \times C(H) \quad (2)$$

κ is a constant in Eq. (2) with small value and the maximum value that $C(H)$ can reach is 0.75.

Using Eqs. (1) and (2) we can express the resistivity for the hydrogen-containing zone as an exponential decay as a function of depth into the foil (z):

$$\rho(z) = \rho_0 + \varepsilon \times e^{-z/\lambda(t)}. \quad (3)$$

Where ρ_0 is the resistivity of pure Pd and ε is the maximum increase in the resistivity due to hydrogen absorption. The resistance of the foil

Table 1
Elemental composition of samples by EDS.

Electron energy (keV)	Depth (μm)	Ru–Pd surface alloy (at.%)				5% Ru–Pd foil (at.%)				Pd foil (at.%)			
		Pd	Ru	O	Others	Pd	Ru	O	Others	Pd	Ru	O	Others
10	0.4	90	10	1	–	–	–	–	–	–	–	–	–
15	0.8	94	6	–	–	–	–	–	–	–	–	–	–
25	1.8	97	0	3	–	84	6	10	–	81	0	18	1

with absorbed hydrogen can be modeled using the contribution of multiple resistance in parallel, each compose by a slab with a thickness Δz and with a hydrogen concentration $C(H)$. The integration of the inverse of the multiple resistances yields the inverse of the total resistance change and if we measure this change we can obtain the parameters ε and λ.

The change in resistance of the Pd foil was measured with a Keithly 580 micro-ohm-meter after dosing with 1000 and 5000 L hydrogen. The resistance change after 1000 L was $\Delta R_1 = 1 \cdot 10^{-5}\ \Omega$ (100 s) and after 5000 L was $\Delta R_2 = 3 \cdot 10^{-5}\ \Omega$ (500 s). The resistance change after 1000 L for the 5% Ru–Pd foil was $\Delta R_3 = 0.4 \cdot 10^{-5}\ \Omega$ and did not change further at 5000 L. The values obtained for Pd foil are: $\lambda_1 = 0.061$ mm; $\lambda_2 = 0.78$ mm. The value obtained for 5% Ru–Pd is $\lambda_3 = 0.023$ mm.

The values of λ obtained for the 1000 L dosage indicate that under this dosage the Pd foil is not saturated with hydrogen (hydrogen diffused less than 1/3 of the total thickness of foil) and the TPD data shows only the kinetics of hydrogen absorption (and desorption) in such a time scale but not the saturation values in equilibrium. In order to obtain the saturation values for pure Pd and for the 5% Ru–Pd alloy, we evaporated these materials on top of quartz crystals and measured the hydrogen uptake as a function of hydrogen pressure.

3.4. "H/M" ratio in Pd films e-beam grown measured by QMC

A 24 nm thick Pd film grown onto the circular quartz crystal (QC) was placed in the QMC head and the flange was sealed to the steel chamber with a Cu gasket. The chamber was pumped down to 1×10^{-4} Pa and the QC resonant frequency was recorded. Then, the chamber was filled with hydrogen reaching a pressure value between 665 and 7315 Pa. This was done by steps of 665 Pa. As soon as hydrogen was allowed to enter the chamber (less than 5 s) at a given pressure, the shifting of QC resonance frequency was recorded for 300 s to make sure that there were no further changes. The same procedure was followed for a 24 nm thick 5% Ru–Pd sample. The 5% Ru–Pd foil was also e-beam evaporated but due to the high melting point of Ru, the film could have been Ru deficient. Plots of QC resonance frequency versus time for the 24 nm thick Pd film and 5% Ru–Pd film at different hydrogen pressures ranging from 665 to 4500 Pa are displayed in Fig. 7. In this plot we can observe that the QC frequency drops (mass gain) down to a constant value (plateau) after 3325 Pa for Pd and around 1995 Pa for 5% Ru–Pd.

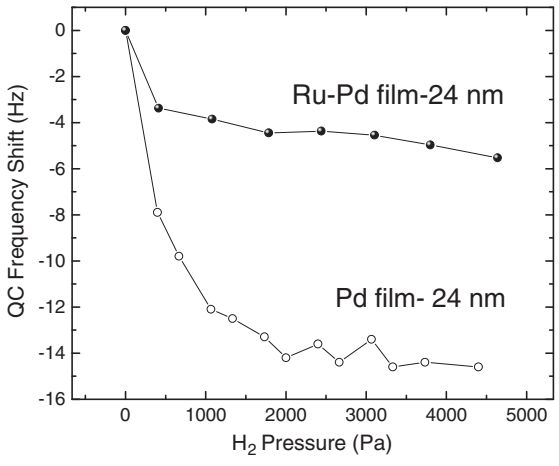

Fig. 7. Plots of QC resonance frequency versus time for the 24 nm thick Pd film and 5% Ru–Pd film at different hydrogen pressures ranging from 665 to 4500 Pa.

The relationship between the mass added or subtracted to the quartz crystal and the shift in its resonance frequency was modeled by Sauerbrey [21] and is represented by the following equation:

$$\Delta f = -\frac{2f^2}{A\sqrt{\delta \times \mu}}\Delta m. \tag{4}$$

Where f is the resonant frequency, δ is the density, μ is the shear modulus of the QC and A is the area covered by the mass. We define the constant C_f:

$$\frac{2f^2}{A\sqrt{\delta \times \mu}} = C_f. \tag{5}$$

Thus:

$$\Delta f = -C_f \Delta m. \tag{6}$$

In order to obtain the constant C_f experimentally, we grew Pd films of different thicknesses and we plotted the Pd mass versus the shift in resonant frequency, obtaining a value for C_f:

$C_f = 1.62 \times 10^{11}(\mathrm{Hz/kg})$ a constant calculated per unit area C_f:*

$$C^*_f = 8.1 \times 10^6 \left(\mathrm{Hz} \times \mathrm{m}^2/\mathrm{kg}\right).$$

This value agrees well with the value of $22.2 \times 10^6(\mathrm{Hz} \times \mathrm{m}^2/\mathrm{kg})$ obtained for a AT-cut, 10 MHz quartz crystal and measured in vacuum and gas phase [22]. If we do the correction of C^* using the resonant frequency ratio we have to multiply 22.2×10^6 by $(6)^2/(10)^2 = 0.36$ which yields the value of $8.0 \times 10^6(\mathrm{Hz} \times \mathrm{m}^2/\mathrm{kg})$.

We then proceed to measure the hydrogen absorption, keeping in mind that the results were not corrected by the effect of stress due to Pd expansion. The total frequency shift for the 24 nm thick Pd film corresponds to about 9.3×10^{-11} kg of hydrogen and for the 5% Ru–Pd foil corresponds to 3.7×10^{-11} kg of hydrogen mass. Since the Pd films were grown on the same QC, we know the Pd mass of the films which was 1.44×10^{-8} kg and thus we can calculate the $x = \frac{H}{Pd}$ atom ratio. For Pd, a ratio of $x = 0.68$ was observed. For the 5% Ru–Pd film a ratio of $x = 0.27$ can be estimated, significantly lower than in the case of Pd.

In order to quantify the amount of Ru in the evaporated film, AES was performed and surface atomic concentration was estimated to be 2.8 at.% Ru. An accurate composition of the Ru–Pd alloy for this 24 nm thick film was impossible to ascertain using EDS because the film was extremely thin. The amount of hydrogen absorbed by pure Pd film resulted 2.5 times larger compared with the amount absorbed by the

Ru–Pd alloy film, in these measurements, at a hydrogen pressure of 4655 Pa.

Frolich et al. [23] measured hydrogen absorption using a volumetric system for 16×10^{-6} m thick Pd and 4% Ru–Pd alloy. The samples were heated to 400 K (100 K above our measurements) and exposed to 1 bar (10^5 Pa) of hydrogen and they found for Pd a ratio of H/M = 0.6 and for 4% Ru–Pd a ratio of H/M = 0.4. Hubkowska et al. [24] measured the hydrogen absorption capacity of a series of electrodeposited Ru–Pd alloy. For a 5.2% Ru they found H/M = 0.58 but this ratio rapidly decreased adding more Ru (H/M ratio of 0.45 for 10% Ru). In both of these measurements [23,24] the Pd films (thickness of the order of 1–16 μm) absorbed 1.6 more hydrogen than a Ru–Pd film (Ru in a range of 4–10%). The amount of hydrogen absorbed by the Ru–Pd alloy is extremely dependent on the Ru composition [24] and a precise composition of the Ru–Pd alloy is needed to being able to correlate with the amount of hydrogen absorbed. At present, it is not our intention to determine with great precision the amount of hydrogen absorbed by each film but to show that in equilibrium the ratio of hydrogen absorption between Pd and the Ru–Pd alloy is much less than the ratio of 12 found in the TPD experiments.

4. Conclusions

The amount of hydrogen evolved from Pd foil after 1000 L dosage in a TPD experiment resulted to be 12 times larger than that for the 5% Ru–Pd foil. A Ru surface alloy of about 1.8 μm thickness grown on the surface of a Pd foil produces a similar effect than the bulk 5% Ru–Pd. The amount of hydrogen absorbed by a 24 nm thickness pure Pd film, measured with QC microbalance, was only less than 2.5 times larger than for the film of the alloy of ~3% Ru–Pd with the same thickness up to a pressure of 4655 Pa. From these results we can conclude that the TPD measurement is diffusion-limited and the QCM measurements are a good indication of hydrogen saturation at equilibrium. Alloying Pd with small amounts of Ru deposited on its surface produced a diffusion barrier for hydrogen absorption and also reduced the saturation solubility of hydrogen in the metal. The "geometric" effect could be responsible for the slower diffusion but clearly an "electronic" effect is responsible for the reduction of the total amount of hydrogen by the metal. It is surprising to observe that a small amount of Ru atoms (less than 5%) replacing Pd in the lattice could have such an effect on the absorption of hydrogen.

Acknowledgments

We acknowledge the support from the Instituto de Física, VRI Puente N° 10/2012 and FONDECyT N° 1130372 and N° 11130555. P. Ferrari and S. Rojas acknowledge CONICyT for scholarship. Thanks are due to M. Soto for SEM and EDS analyses and R. El Far for XRD analyses.

References

[1] F.A. Lewis, The Palladium Hydrogen System, Academic Press, New York, 1967.
[2] A. Czerwinski, Pol. J. Chem. 69 (1995) 699.
[3] J.N. Armor, Chemtech 22 (1992) 557.
[4] R.J. Behm, V. Penka, M.G. Cattania, K. Christmann, G.J. Ertl, Chem. Phys. 78 (1983) 7486.
[5] C.P. Romero, R.A. Trabol, J.I. Avila, P. Lievens, A.L. Cabrera, Int. J. Hydrogen Energy 36 (2011) 13595.
[6] A.L. Cabrera, E. Morales-Leal, J. Hasen, I.K. Schuller, Catal. Lett. 30 (1995) 11.
[7] M. Lukaszewski, M. Grden, A. Czerwinski, J. New Mater. Electrochem. Syst. 9 (2006) 409.
[8] X. Ke, G.J. Kramer, O.M. Lovvik, J. Phys. Condens. Matter 16 (2004) 6267.
[9] C.L. Wang, J. Krim, M.F. Toney, J. Vac. Sci. Technol. A 7 (3) (1989) 2481.
[10] J. Krim, D.H. Solina, R. Chiarello, Phys. Rev. Lett. 66 (2) (1991) 181.
[11] J. Krim, C. Daly, Handbook of Thin Films Process Technology, IOP Publishing Ltd., 1995. (Chapt. D4.0).
[12] "QCM100-Quartz Crystal Microbalance: Theory and Calibration", Application Notes, Stanford Research Systems, 2013. (www.thinkSRS.com).
[13] M. Grden, J. Kotwski, A. Czerwinski, J. Solid State Electrochem. 4 (2004) 273.
[14] M. Lukaszewki, A. Czerwinski, J. Electroanal. Chem. 589 (2006) 87.
[15] R. El Far, D.E. Diaz-Droguett, S. Rojas, J.I. Avila, C.P. Romero, P. Lievens, A.L. Cabrera, Thin Solid Films 522 (2012) 199.
[16] A.E. Ribbe, Inst. Sci. Technol. 34 (2006) 501.
[17] K. Kanaya, S. Okayama, J. Phys. D. Appl. Phys. 5 (1972).
[18] A.L. Cabrera, R. Aguayo-Soto, Catal. Lett. 45 (1997) 79.
[19] E. Johansson, S. Olsson, C. Chacon, B. Hjorvarsson, J. Phys. Condens. Matter 16 (2004) 1165.
[20] M.A. Pick, J.W. Davenport, M. Strongin, G.J. Dienes, Phys. Rev. Lett. 43 (1979) 286.
[21] T.G. Sauerbrey, Z. Phys. 155 (1959) 206.
[22] Michael Rodahl, Fredrik Hook, Anatol Krozer, Peter Brzezinski, Bengt Kasemo, Rev. Sci. Instrum. 66 (7) (1995) 3924.
[23] K. Frolich, H.G. Severin, R. Hempelmann, E. Wicke, Z. Phys. Chem. N.F. Bd. 119 (1980) S. 33.
[24] K. Hubkowska, M. Lukaszewski, A. Czerwinski, Electrochem. Commun. 20 (2012) 175.